Measurement of the parity violating asymmetry in the quasielastic electron-deuteron scattering and improved determination of the magnetic strange form factor and the isovector anapole radiative correction

Citation: Balaguer Ríos, D., et al. "Measurement of the Parity Violating Asymmetry in the Quasielastic Electron-Deuteron Scattering and Improved Determination of the Magnetic Strange Form Factor and the Isovector Anapole Radiative Correction." Physical Review D, vol. 94, no. 5, Sept. 2016. © 2016 American Physical Society

As Published: http://dx.doi.org/10.1103/PHYSREVD.94.051101

Publisher: American Physical Society (APS)

Persistent URL: http://hdl.handle.net/1721.1/116715

Version: Final published version: final published article, as it appeared in a journal, conference proceedings, or other formally published context

PHYSICAL REVIEW D **94,** 051101(R) (2016)

Measurement of the parity violating asymmetry in the quasielastic electron-deuteron scattering and improved determination of the magnetic strange form factor and the isovector anapole radiative correction

D. Balaguer Ríos,[1,†] K. Aulenbacher,[1] S. Baunack,[1] J. Diefenbach,[1] B. Gläser,[1] D. von Harrach,[1] Y. Imai,[1] E.-M. Kabuß,[1] R. Kothe,[1] J. H. Lee,[1] H. Merkel,[1] M. C. Mora Espí,[1] U. Müller,[1] E. Schilling,[1] C. Weinrich,[1] L. Capozza,[2] F. E. Maas,[2] J. Arvieux,[3,*] M. A. El-Yakoubi,[3] R. Frascaria,[3] R. A. Kunne,[3] S. Ong,[3] J. van de Wiele,[3] S. Kowalski,[4] and Y. Prok[4]

[1]*Institut für Kernphysik, Johannes Gutenberg-Universität Mainz, J.J. Becherweg 45, D-55099 Mainz, Germany*

[2]*Helmholtz-Institut Mainz, Johannes Gutenberg-Universität Mainz, J.J. Becherweg 36, D-55099 Mainz, Germany*

[3]*Institut de Physique Nucléaire, CNRS-IN2P3, Université Paris-Sud, F-91406 Orsay Cedex, France*

[4]*Laboratory for Nuclear Science and Department of Physics, MIT, Cambridge, Massachusetts 02139, USA*

(Received 19 April 2016; published 12 September 2016)

A new measurement of the parity-violating asymmetry in the electron-deuteron quasielastic scattering for backward angles at $\langle Q^2 \rangle = 0.224\ (\mathrm{GeV}/c)^2$, obtained in the A4 experiment at the Mainz Microtron accelerator (MAMI) facility, is presented. The measured asymmetry is $A_{PV}^d = (-20.11 \pm 0.87_{\mathrm{stat}} \pm 1.03_{\mathrm{sys}}) \times 10^{-6}$. A combination of these data with the proton measurements of the parity-violating asymmetry in the A4 experiment yields a value for the effective isovector axial-vector form factor of $G_A^{e,(T=1)} = -0.19 \pm 0.43$ and $R_A^{(T=1),\mathrm{anap}} = -0.41 \pm 0.35$ for the anapole radiative correction. When combined with a reanalysis of measurements obtained in the G0 experiment at the Thomas Jefferson National Accelerator Facility, the uncertainties are further reduced to $G_M^s = 0.17 \pm 0.11$ for the magnetic strange form factors, and $R_A^{(T=1),\mathrm{anap}} = -0.54 \pm 0.26$.

DOI: 10.1103/PhysRevD.94.051101

The most remarkable feature of the strong interaction at low energies is confinement. Its effect, however, cannot be calculated using perturbative methods of the QCD theory. The QCD degrees of freedom, the quarks, are present as hadrons—mesons and baryons. Among the baryons, the proton is the ground state. Its structure can be understood in terms of the valence quarks and the quark sea, consisting of quark-antiquark pairs that involve mainly the three light quarks u, d and s. The strange quark s in the proton is then a pure quark sea effect. Parity-violation experiments have been the tool of choice for exploring the vector-matrix elements of the strange quark [1]. The parity-violating asymmetry contains electroweak radiative corrections that exhibit the same kinematic dependence as the nucleon axial-vector form factor. These radiative corrections can be large; in particular, the anapole radiative correction depends strongly on the hadronic structure, as it arises from the coupling of the virtual photon to axial-vector currents originating from the internal electroweak dynamics of the nucleon [2–4].

The contribution of the strange quark ($G_{E,M}^s$) to the nucleon electromagnetic form factors $G_{E,M}^{p,n}$ can be determined from the neutral weak form factors [5]. These form factors can be obtained by measuring the parity-violating asymmetry in elastic electron-proton scattering. Through a combination of two measurements of the parity-violating asymmetry at the same Q^2, the electric and magnetic strange form factors G_E^s and G_M^s can be separated [1], if the effective axial-vector form factor $G_A^{e,p}$ is introduced as an input [6]. A third measurement of the parity-violating asymmetry in the quasielastic electron-deuteron scattering at backward angles will then isolate the effective isovector axial-vector form factor $G_A^{e,(T=1)}$.

Here we present the analysis of a new measurement of the parity-violating asymmetry at $\langle Q^2 \rangle = 0.224\ (\mathrm{GeV}/c)^2$ and an average $\bar{\theta} = 145°$, obtained in the A4 experiment at the Mainz Microtron (MAMI). In addition, a recent lattice-QCD calculation is used to separate the effective isovector axial-vector form factor $G_A^{e,(T=1)}$ from its isoscalar counterpart, $G_A^{e,(T=0)}$ [7]. The combination of the A4 results presented here with asymmetries measured previously in the A4 experiment [6,8], and with the asymmetries obtained in the G0 experiment at the Thomas Jefferson National Accelerator Facility [9,10], leads to a substantial reduction of the experimental uncertainty for the values of $G_A^{e,(T=1)}$ and of G_M^s. The anapole radiative correction is extracted and compared to the theoretical calculations of Zhu *et al.* [2]. This radiative correction contains hadronic effects. The determination of these radiative corrections has an important role in high-precision determinations of the weak mixing angle $\sin^2\theta_W$ at very low Q^2, as is planned in the P2 experiment in Mainz [11].

*Deceased.
†dabarios@kph.uni-mainz.de

The parity-violating asymmetry can be decomposed into three terms: $A_{PV} = A_V + A_S + A_A$ [1], where the subscript V refers to the vector coupling to the nucleon without strangeness, S to the vector coupling of the strange quark, and A to the axial-vector coupling of the nucleon. The difference between the measured value of A_{PV} and the theoretical expectation for A_V gives a term that depends on G_E^s, G_M^s and $G_A^{e,p}$. For the proton,

$$A_{PV}^p - A_V^p = a\frac{\epsilon G_E^p G_E^s + \tau G_M^p G_M^s + g_v \epsilon' \tau' G_M^p G_A^{e,p}}{\sigma_p^r}, \quad (1)$$

where $a = \frac{G_F Q^2}{4\pi\alpha\sqrt{2}}$ with G_F being the Fermi coupling constant, $\sigma_p^r = \epsilon(G_E^p)^2 + \tau(G_M^p)^2$ with $\epsilon = (1+2(1+\tau)\tan^2\theta/2)^{-1}$, $\tau = Q^2/4M_N^2$ with M_N being the nucleon mass, $g_v = 1 - 4\sin^2\theta_W$, $\epsilon' = \sqrt{1-\epsilon^2}$, and $\tau' = \sqrt{\tau(1+\tau)}$. The radiative corrections in the tree-level equation (1) have been taken into account; see Ref. [1].

The parity-violating asymmetry in the electron-deuteron quasielastic scattering separates $G_A^{e,(T=1)}$ from $G_A^{e,(T=0)}$:

$$A_{PV}^d - A_V^d = a\frac{\epsilon(G_E^p + G_E^n)G_E^s + \tau(G_M^p + G_M^n)G_M^s + g_v\epsilon'\tau'[(G_M^p - G_M^n)G_A^{e,(T=1)} + (G_M^p + G_M^n)G_A^{e,(T=0)}]}{\sigma_p^r + \sigma_n^r}, \quad (2)$$

where $\sigma_n^r = \epsilon(G_E^n)^2 + \tau(G_M^n)^2$.

$G_A^{e,(T=0)}$ and $G_A^{e,(T=1)}$ are parametrized as follows:

$$G_A^{e,(T=0)} = (-g_A R_A^{e,(T=0)} + \Delta s)G_A^D, \quad (3)$$

$$G_A^{e,(T=1)} = -g_A[(1 + R_A^{e,(T=1)})]G_A^D, \quad (4)$$

$$G_A^D = \left(1 + \frac{Q^2}{M_A^2}\right)^{-2}, \quad (5)$$

where $R_A^{(T=0)}$ and $R_A^{(T=1)}$ are the isoscalar and isovector electroweak radiative corrections, respectively; $M_A = (1.026 \pm 0.021)\ \mathrm{GeV}/c^2$ is the axial mass [12]; $g_A = 1.2723(23)$ is the nucleon axial coupling due to the neutron beta decay [13]; and $\Delta s = -0.13 \pm 0.13$ is the strange-quark contribution to the nucleon polarization [14].

Each component $R_A^{(T=i)}$, with $i = 0, 1$, is the sum of one-quark and multiquark (anapole) radiative corrections $R_A^{(T=i)} = R_A^{(T=i),1q} + R_A^{(T=i),\mathrm{anap}}$. The $R_A^{(T=i),1q}$ values are calculated from one-quark diagrams within the Standard Model, whereas $R_A^{(T=i),\mathrm{anap}}$ values are calculated from multi-quark diagrams using the heavy baryon chiral perturbation theory (HBχPT) [2,3,15] and the chiral quark model (χQM) [4]. The calculations of $R_A^{(T=i),\mathrm{anap}}$ are affected by large theoretical uncertainties related to the lack of knowledge about the parity-violating meson-nucleon couplings [2–4,15]. In Eq. (2), we assume the static approximation. There are calculations that have taken into account the coherent scattering on the deuteron, including two-body current operators [16] and parity-violating nucleon-nucleon interactions [17,18]. The systematic error associated with assuming the static approximation has been estimated to be at the level of 1% [19] for the A4 kinematics, and it is included in the extraction of the form factors and the anapole radiative correction.

The experimental setup used in the A4 experiment [6,8,20–27] at MAMI is described in detail in Ref. [8]. In short, the accelerator provides a high-quality, longitudinally polarized electron beam with up to 80% polarization, a current of 20 μA and a beam energy of 315.1 MeV. The data were taken alternately with and without insertion of a $\lambda/2$ wave plate in the polarized electron-beam source ("in"/"out"). The $\lambda/2$ wave plate suppresses systematic effects and serves to systematically test the correct change of sign for the physical parity-violating asymmetry. False asymmetries originate from helicity-correlated beam differences of energy, position, angle and intensity. Several feedback loops stabilize these beam parameters.

Once the beam reaches the A4 experiment, it passes with a luminosity of $1.4 \times 10^{38}\ \mathrm{cm}^{-2}\,\mathrm{s}^{-1}$ through a liquid deuterium target [26]. The scattered electrons are registered in a homogeneous, segmented, totally absorbing electromagnetic PbF_2 calorimeter [22] that is mounted on a rotatable platform and can be operated at both forward and backward angles. The calorimeter is composed of 1022 crystals arranged in 146 slices and 7 rings. They cover the 2π azimuthal angle and the polar-angle interval $[140°, 150°]$. The energy resolution is $3.9\%/\sqrt{E(\mathrm{GeV})}$, which is enough to separate elastically scattered from inelastically scattered electrons. The signals are digitized using fast electronics with a single-channel dead time of 20 ns and are stored as histograms. Individual events are counted in the histogram. In the backward configuration, an additional detector consisting of plastic scintillators discriminates between charged and neutral particles, separating scattered electrons from photons originating from π^0 decays. For each of the 1022 channels, four histograms of the detected events are stored on disk every five minutes. For each polarization state $(+,-)$, an energy spectrum for charged particles $(A+, A-)$ and a spectrum for neutral particles $(B+, B-)$ is generated; see Fig. 1.

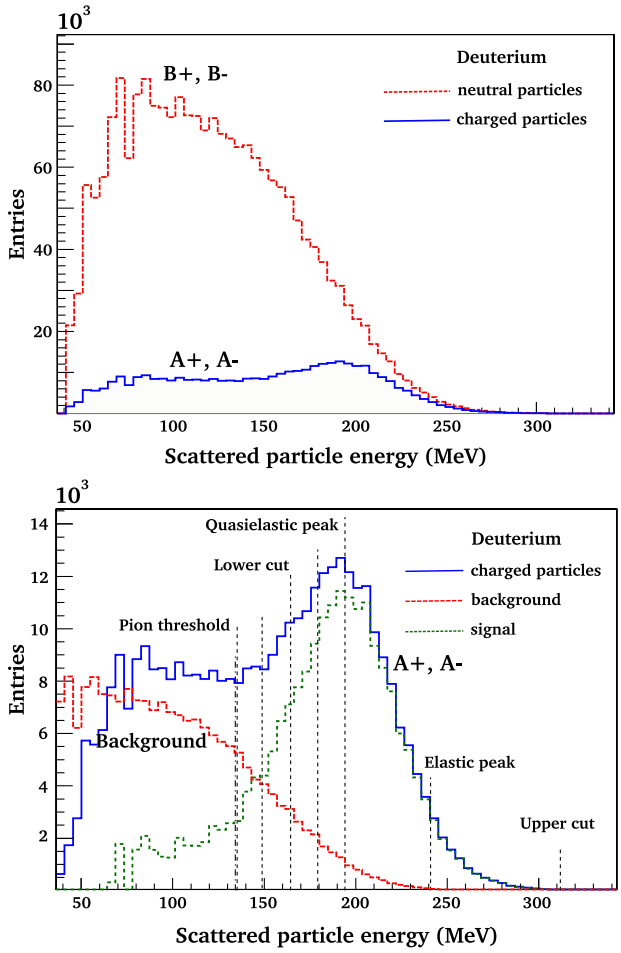

FIG. 1. Upper panel: Experimentally obtained energy spectra of neutral particles B (dashed line) and charged particles A (solid line). Lower panel: The spectrum of charged particles A (solid line), the background from the γ conversion in A (dashed line) and the spectrum A with subtracted background (dotted line). Vertical lines mark the positions of the quasielastic peak, the elastic peak, the upper cut, the lower cuts (dashed lines) and the pion-production threshold (dot-dashed lines).

In the spectrum $(A+, A-)$, the quasielastic peak from scattering off deuterium is clearly visible (Fig. 1). It is broadened due to Fermi motion. A Gaussian function is fitted to the right slope of this spectrum to obtain the mean value of the peak, μ, and its width, σ. This spectrum contains background contributions from the conversion of high-energy photons in the aluminum of the scattering chamber and in the plastic scintillators in front of the calorimeter. The parity-violating asymmetry A_e is extracted from $(A+, A-)$ through counting the number of scattered particles under the quasielastic peak, by integrating between a lower-cut value c_l and an upper-cut value c_u. The parity-violating asymmetry of the background A_γ is obtained from $(B+, B-)$. These asymmetries are averaged over the five inner rings of the detector, weighted by their respective cross sections. The method for the correction of the background asymmetry is explained in detail in Ref. [6]. The correction for the background with a dilution factor f is

$$A_{PV}^{i,j,k} = \frac{A_e^{i,j,k} - f A_\gamma^{i,j,k}}{1-f}, \qquad A_{PV}^{i,k} = \frac{1}{N}\sum_j A_{PV}^{i,j,k}, \tag{6}$$

where the superscript i labels the slice, j the five-minute run and k the 70-hour sample of asymmetries, with and without insertion of the $\lambda/2$ wave plate in the polarized electron-beam source ("in"/"out"). N stands for the number of runs. $A_{PV}^{i,j,k}$ is averaged over all runs j to obtain $A_{PV}^{i,k}$. A_{PV}^{i} is calculated with an error-weighted average over the $\lambda/2$ wave plate samples k of $A_{PV}^{i,k}$, changing the sign for the "in" samples. Finally, A_{PV} is obtained by averaging over the slices i. To optimize statistical precision and minimize systematic uncertainty from the background, several $c_l = \mu - \kappa\cdot\sigma$ $(\kappa = 2, \ldots, 0)$ are tested, with fixed $c_u = \mu + 3.0\sigma$. An optimal c_l with $\kappa = 1.5$ minimizes ΔA_{PV}. A_{PV} displays no significant dependence on c_l.

The parity-violating asymmetry is corrected for other sources of background contributions that have their own asymmetries: the quasielastic scattering on the aluminum windows possesses parity-violating asymmetry A_a with a dilution factor g, the random-coincidence events in the plastic scintillators have A_r with dilution factor h, and the electron-deuteron elastic scattering exhibits have A_η with dilution factor η. These background sources have been corrected globally. The corrections have been calculated from the difference

$$\frac{A_{PV}(1-f) - gA_a - hA_r - \eta A_\eta}{1-f-g-h-\eta} - A_{PV} \tag{7}$$

as f is dominant. The aluminum background is estimated from a measurement of the energy spectrum with empty target. A_a is calculated assuming the static approximation, using A_V^p and A_V^n. The random-coincidence background is determined from $(B+, B-)$, and A_r is compatible with zero. The background from the electron-deuteron elastic

TABLE I. Systematic corrections to the asymmetry and their contribution to the systematic uncertainty.

	Scaling factor	Error (ppm)
Polarization	0.74	0.75
	Correction (ppm)	Error (ppm)
Dilution of γ backgr.	−3.07	0.67
Helicity corr. beam diff	0.24	0.16
Al windows	0.01	0.06
Random-coinc. events	−0.61	0.10
Elastic scattering	−0.14	0.04
Target density	−0.81	0.06
Sum syst. errors		1.03

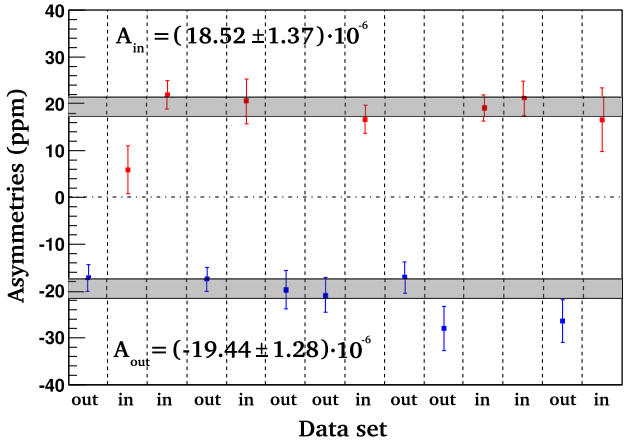

FIG. 2. Samples of the extracted asymmetries A_{PV}^{k}, taken with ("in") or without ("out") a $\lambda/2$ wave plate in the electron-beam source. The asymmetries exhibit the change of sign expected for a parity-violating asymmetry. The fits to the "out" samples, $A_{\text{out}} = (-19.44 \pm 1.28) \times 10^{-6}$; the "in" samples, $A_{\text{in}} = (18.52 \pm 1.37) \times 10^{-6}$; and to the combined data, $A = (-19.01 \pm 0.94) \times 10^{-6}$ are consistent within the error bars. The shaded bands mark the 1σ width for the fit to the combined asymmetry samples.

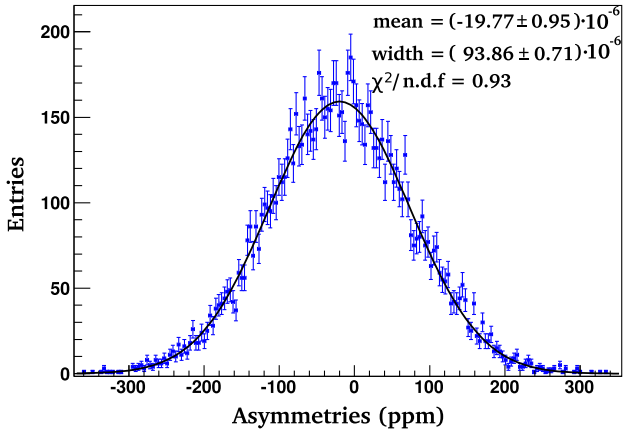

FIG. 3. Histogram of the extracted asymmetries A_{PV}^{j}. A Gaussian function has been fitted to the histogram (solid line). The goodness of the fit confirms that the histogram of A_{PV}^{j} follows a normal probability distribution.

scattering is estimated from the cross section calculated with a phenomenological parametrization of the three electromagnetic form factors of the deuteron [28]. A_η without strangeness is obtained from Ref. [29]. A_{PV}^{i} is corrected for target-density fluctuations and for the false asymmetries from helicity-correlated beam differences in the energy, position, angles and current, applying a multilinear regression method. The set of systematic corrections and uncertainties is summarized in Table I.

Several systematic tests show that A_{PV} is the physical parity-violating asymmetry. A_{PV}^{i} shows no significant dependence on the azimuthal angle. A_{PV}^{k} exhibits the change of sign expected for a parity-violating asymmetry under the insertion of a $\lambda/2$ wave plate in the polarized electron-beam source (Fig. 2). A normal probability distribution has been fitted to the experimental sample of A_{PV}^{j}; see Fig. 3.

The three measurements in the A4 experiment at $\langle Q^2 \rangle = 0.224$ $(\text{GeV}/c)^2$, two of A_{PV}^{p} at forward and backward angles [6,8] and A_{PV}^{d} presented in this paper, are sufficient to determine $G_A^{e,(T=1)}$ and to extract $R_A^{(T=1),\text{anap}}$ by subtracting $R_A^{(T=1),1q}$ [2]. We obtain

$$G_A^{e,(T=1)} = -0.19 \pm 0.27_{\text{stat}} \pm 0.31_{\text{syst}} \pm 0.12_{\text{th}},$$
$$R_A^{(T=1),\text{anap}} = -0.41 \pm 0.22_{\text{stat}} \pm 0.26_{\text{syst}} \pm 0.08_{\text{th}}.$$

A recent lattice-QCD calculation of G_E^s [7] is used to determine G_M^s and $G_A^{e,(T=0)}$ and thereby $R_A^{(T=0),\text{anap}}$:

$$G_M^s = 0.43 \pm 0.27_{\text{stat}} \pm 0.16_{\text{syst}} \pm 0.03_{\text{th}},$$
$$G_A^{e,(T=0)} = -2.15 \pm 1.03_{\text{stat}} \pm 0.81_{\text{syst}} \pm 0.01_{\text{th}},$$
$$R_A^{(T=0),\text{anap}} = 1.62 \pm 0.84_{\text{stat}} \pm 0.65_{\text{syst}} \pm 0.07_{\text{th}}.$$

The first error originates from the statistical error of the asymmetries, the second from the systematic uncertainties, and the third from theory.

A further reanalysis was performed for the published data of the G0 experiment [9,10]. The set of three asymmetries for each Q^2 have been used to determine G_M^s, $G_A^{e,(T=1)}$, $G_A^{e,(T=0)}$, $R_A^{(T=1),\text{anap}}$ and $R_A^{(T=0),\text{anap}}$ using the lattice-QCD calculation of G_E^s [7] instead of the theoretical calculation of $R_A^{(T=0)}$ [2]. The experimental uncertainties have been reduced using $G_{E,M}^{p,n}$ obtained in a Monte Carlo analysis of the world data [30] instead of the Kelly parametrization used by G0 [9,10]. The results of the reanalysis, together with the results of the A4 experiment,

TABLE II. List of form factors and anapole radiative corrections from the A4 and G0 experiments, using the lattice-QCD value for G_E^s [7]. The statistical, systematic and theoretical errors have been added in quadrature.

Experiment	Q^2 $(\text{GeV}/c)^2$	G_M^s	$G_A^{e,(T=1)}$	$G_A^{e,(T=0)}$	$R_A^{(T=1),\text{anap}}$	$R_A^{(T=0),\text{anap}}$
A4	0.224	0.43 ± 0.32	-0.19 ± 0.43	-2.15 ± 1.31	-0.41 ± 0.35	1.65 ± 1.06
G0	0.221	-0.19 ± 0.19	-0.60 ± 0.36	0.95 ± 0.87	-0.09 ± 0.29	-1.15 ± 1.00
G0	0.628	0.16 ± 0.07	-0.25 ± 0.36	-1.23 ± 0.64	-0.22 ± 0.50	2.40 ± 1.27

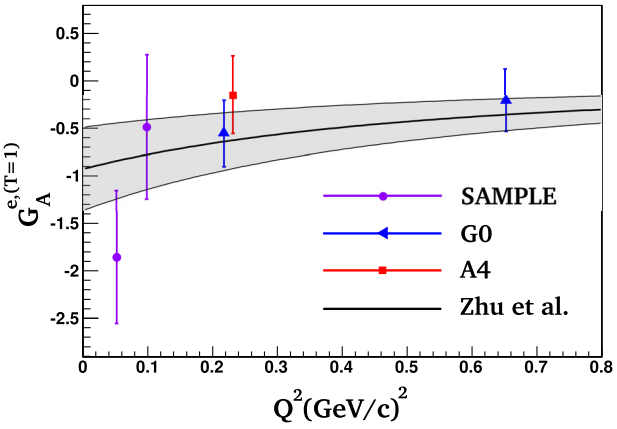

FIG. 4. Experimental determinations of the isovector axial-vector form factors from the A4 (square), the G0 (triangle) and the SAMPLE (circle) experiments at different Q^2. The theoretical calculation of Zhu *et al.* [2] is shown as a solid line, assuming a Q^2 dipole dependence of the axial mass. The gray band marks the 1σ uncertainty interval.

are shown in Table II. The statistical, systematic and theoretical errors have been added in quadrature.

The extracted quantities based on the measurements obtained in the A4, G0 [9,10] and SAMPLE (at the MIT Bates lab [31]) experiments of $G_A^{e,(T=1)}$ at different Q^2 and the calculation of Zhu *et al.* [2], assuming a Q^2 dipole dependence with the axial mass [12], are shown in Fig. 4. These quantities agree with the theoretical expectation values within the error bars and exhibit a consistent Q^2 dependence.

The extracted quantities shown in Table II are combined to reduce the errors of G_M^s, $G_A^{e,(T=1)}$ and $G_A^{e,(T=0)}$, and therefore $R_A^{(T=1),\mathrm{anap}}$ and $R_A^{(T=0),\mathrm{anap}}$. G_M^s is assumed to follow a Q^2 dipole dependence with the vector mass, and $G_A^{e,(T=1)}$ and $G_A^{e,(T=0)}$ a Q^2 dipole dependence with the axial mass [12], including the radiative corrections. This results in a positive $\mu^s = G_M^s(0) = 0.30 \pm 0.19$, with a quality of the fit given by $\chi^2/\mathrm{n.d.f.} = 2.77$ at more than 1σ from zero. [The number of degrees of freedom (n.d.f.) is 2, here and in the fits discussed below.] Extrapolation to $\langle Q^2 \rangle = 0.224\ (\mathrm{GeV}/c)^2$ yields $G_M^s = 0.17 \pm 0.11$. The error 0.11 is by a factor of $\sim\sqrt{2}$ smaller than the error from the hydrogen measurements in the A4 experiment [6]. The fit to the axial-mass Q^2 dependence yields $G_A^{e,(T=1)}(0) = -0.59 \pm 0.34$, with a good fit quality, $\chi^2/\mathrm{n.d.f} = 0.29$, and $G_A^{e,(T=0)}(0) = -0.90 \pm 0.82$ with $\chi^2/\mathrm{n.d.f.} = 3.29$. The extracted anapole radiative corrections are $R_A^{(T=1),\mathrm{anap}} = -0.54 \pm 0.26$ and $R_A^{(T=0),\mathrm{anap}} = 0.62 \pm 0.65$. The error of $R_A^{(T=1),\mathrm{anap}}$ is slightly larger than the theoretical uncertainty [2], and $R_A^{(T=0),\mathrm{anap}}$ exhibits a large error and a positive value compatible with zero.

In summary, a combination of measurements of A_{PV} obtained in the A4 experiment at the same Q^2 (forward H_2, backward H_2 and backward D_2) has been used to determine $G_A^{e,(T=1)}$ and $R_A^{(T=1),\mathrm{anap}}$. The values G_M^s, $G_A^{e,(T=0)}$ and $R_A^{(T=0),\mathrm{anap}}$ were determined using as theoretical input the lattice-QCD calculation of G_E^s [7]. Combination with the quantities obtained from a reanalysis of the G0 data [9,10] enabled a reduction of the experimental uncertainties.

Future measurements of A_{PV} in the A4 experiment at $Q^2 = 0.1\ (\mathrm{GeV}/c)^2$ will help to further reduce the errors of G_M^s, $G_A^{e,(T=1)}$, $G_A^{e,(T=0)}$, $R_A^{(T=1),\mathrm{anap}}$ and $R_A^{(T=0),\mathrm{anap}}$. Planned measurements of A_{PV} at very low Q^2 in the P2 experiment at Mainz with improved statistics and systematics will lead to determinations with considerably smaller uncertainties.

ACKNOWLEDGMENTS

This work has been supported by the Deutsche Forschungsgemeinschaft (DFG) within the projects SFB 443, SFB 1044 and the PRISMA excellence cluster. We would like to thank the crew of the MAMI accelerator for the high beam quality.

[1] M. J. Musolf, T. W. Donnelly, J. Dubach, S. J. Pollock, S. Kowalski, and E. J. Beise, Phys. Rep. **239**, 1 (1994).
[2] S. L. Zhu, S. J. Puglia, B. R. Holstein, and M. J. Ramsey-Musolf, Phys. Rev. D **62**, 033008 (2000).
[3] C. M. Maekawa, and U. van Kolck, Phys. Lett. B **478**, 73 (2000).
[4] D. O. Riska, Nucl. Phys. **A678**, 79 (2000).
[5] D. B. Kaplan, and A. Manohar, Nucl. Phys. **B310**, 527 (1988).
[6] S. Baunack *et al.*, Phys. Rev. Lett. **102**, 151803 (2009).
[7] J. Green, S. Meinel, M. Engelhardt, S. Krieg, J. Laeuchli, J. Negele, K. Orginos, A. Pochinsky, and S. Syritsyn, Phys. Rev. D **92**, 031501 (2015).
[8] F. E. Maas *et al.*, Phys. Rev. Lett. **93**, 022002 (2004).
[9] D. S. Armstrong *et al.*, Phys. Rev. Lett. **95**, 092001 (2005).
[10] D. Androić *et al.*, Phys. Rev. Lett. **104**, 012001 (2010).
[11] D. Becker, S. Baunack, and F. E. Maas, Hyperfine Interact. **214**, 141 (2013).
[12] V. Bernard, L. Elouadrhiri, and U.-G. Meißner, J. Phys. G **28**, R1 (2002).
[13] K. A. Olive *et al.*, Chin. Phys. C **38**, 090001 (2014).

[14] E. Leader, A. V. Sidorov, and D. B. Stamenov, Phys. Rev. D **91**, 054017 (2015).
[15] M. J. Musolf, Phys. Lett. B **242**, 461 (1990).
[16] L. Diaconescu, R. Schiavilla, and U. van Kolck, Phys. Rev. C **63**, 044007 (2001).
[17] R. Schiavilla, J. Carlson, and M. Paris, Phys. Rev. C **67**, 032501 (2003).
[18] C. P. Liu, G. Prézeau, and M. J. Ramsey-Musolf, Phys. Rev. C **67**, 035501 (2003).
[19] R. Schiavilla (private communication).
[20] S. Köbis *et al.*, Nucl. Phys. **61B**, 625 (1998).
[21] P. Achenbach *et al.*, Nucl. Instrum. Methods Phys. Res., Sect. A **416**, 357 (1998).
[22] P. Achenbach, S. Baunack, K. Grimm, T. Hammel, D. von Harrach, A. L. Ginja, F. E. Maas, E. Schilling, and H. Ströher, Nucl. Instrum. Methods Phys. Res., Sect. A **465**, 318 (2001).
[23] F. E. Maas *et al.*, Phys. Rev. Lett. **94**, 082001 (2005).
[24] F. E. Maas *et al.*, Phys. Rev. Lett. **94**, 152001 (2005).
[25] T. Hammel *et al.*, Nucl. Instrum. Methods Phys. Res., Sect. A **564**, 1 (2006).
[26] I. Altarev *et al.*, Nucl. Instrum. Methods Phys. Res., Sect. A **564**, 13 (2006).
[27] S. Baunack *et al.*, Nucl. Instrum. Methods Phys. Res., Sect. A **640**, 58 (2011).
[28] E. Tomasi-Gustafson, Phys. Rev. C **73**, 045204 (2006).
[29] S. J. Pollock, Phys. Rev. D **42**, 3010 (1990).
[30] M. A. Yakoubi *et al.*, in *Proceedings of 3rd Workshop on Parity Violation PAVI 2006*, edited by S. Kox *et al.* (SIF and Springer-Verlag, Berlin, 2007).
[31] T. M. Ito *et al.*, Phys. Rev. Lett. **92**, 102003 (2004).